Optimisation of power cable ampacity in offshore wind farm applications

Optimisation of power cable ampacity in offshore wind farm applications

M Høyer-Hansen, S M Hellesø, K T Solheim, E B Mehammer, E Eberg and P A Pedersen

SINTEF Energy Research, 7034 Trondheim, Norway

Martin.Hoyer-Hansen@sintef.no

Abstract. Inter-array power cables are used to connect wind turbines to the collector and export cable. In the transition from turbine tower to sea, the cable is installed in a J-tube, which has an unfavourable thermal environment and can thus be the thermal bottleneck of the cable installation. To optimize cable installation and reduce CAPEX, improved transient ampacity calculations can be used to determine the dynamic rating. In this work FEM have been applied to calculate the ampacity of a three-core HV cable situated in a J-tube. It was found that by including the trajectory of solar influx, the maximum temperature increased above the admittable cable core temperature compared to the steady-state case. High cable loads will always coincide with wind and thus increased convective heat transfer. By increasing the heat transfer coefficient to a value corresponding to wind speed of 20 m/s at high power production and thus large current, it was found the highest core cable temperature decreased by 18 ºC compared to the steady-state case. These more accurate ampacity calculations can be exploited by either increasing the admissible current in the cable by 17% or decreasing the cable cross section.

1. Introduction

Inter-array and transmission cables account for 25 % of the levelized cost of energy (LCOE) in offshore wind projects [1]. This share is expected to increase to 45 % by 2030, due to increased distance from shore and deeper water. By improving the accuracy of both computational methods and input parameters, the current rating (ampacity) of the cables could be increased, yielding a significant decrease in LCOE.

For wind farm applications, the ampacity is thermally limited. Above the rated ampacity, transport of heat generated by losses in the cable and to the surroundings is not sufficient to avoid overheating of the polymeric insulation. Ampacity calculations are normally done according to IEC 60287 [2] for static loads, while IEC 60853 [3] considers cyclic and emergency loads. Selecting a suitable cable design can thus be viewed as an optimization exercise which depends on several variables, including power production profiles, cable conductor size, and temperature conditions. In an optimal cable installation, the installation cost is balanced with the cost of losses. To find the balance point, accurate electro-thermal models of the cable construction and the surroundings where the cable is installed are required in combination with the expected load profile.

As a first step in cable dimensioning, an expected load profile must be established, which in all cases will be uncertain. A methodology to describe the worst-case dynamic load profile have been demonstrated in [4]. By using this method, a step-load curve is established so that ampacity calculations can readily be done using IEC 60853 and finite element methods (FEM). Catmull *et al.* have estimated simplified cyclic time-current series based on mesoscopic weather models [5], [6]. Ampacity calculations for cyclic loads based on IEC 60853 provides an increase of admittable current of 22 % compared to the static case, although production curtailment is not taken into account in case of long periods of high-power production. For this, Colin and Pilgrim have proposed a methodology to estimate risk of overheating in case of overplanting of wind farms [3]. The dynamic model provides real-time thermal rating and estimates the future load based on historical data and statistics.

A prerequisite to evaluate the thermal risk is determination of the thermal bottleneck along the cable installation, and provide accurate, time-dependent temperature calculations for these. J-tubes and landfalls have been identified as thermal bottlenecks in many cases [7]. With dynamic loads and the potentially deep burial of landfalls, a large increase in admittable current can be expected due to the long thermal time constant [4].

The thermal model must both reproduce the heating in the cable, accounting for losses in the conductor, screen and armouring, and the heat transfer from the cable to the surrounding media. It is important to identify the limitations and bottlenecks during design to be able to select a cost-effective design and to prevent overheating and damaging the cables.

This paper presents electro-thermal computations of power cables modelled using FEM. The models show the importance of selecting the correct cable design, as well as incorporating relevant boundary conditions such as sun exposure, wind cooling, and blackbody radiation. It also shows that a method for considering the cyclic nature of the environmental conditions can greatly increase the available cable ampacity. A proper accounting of the cost/benefit of actual available ampacity and eventual increase of the ampacity by design changes would enable optimal selection of cable infrastructure.

2. Heat transport in offshore wind applications

There are three mechanisms for heat transfer between a cable and a J-tube, and between a J-tube and the surroundings: conduction, convection, and radiation. The heat transfer by conduction is, in principle, given by the following differential equation:

$$\boldsymbol{q} = -k\boldsymbol{\nabla}T \tag{1}$$

where:
$\boldsymbol{q}$ is the vector of the heat flux (W/m^2),
k is the thermal conductivity (W/m.K), and
$\boldsymbol{\nabla}T$ is the gradient operator on the temperature field T (K).

For some simple geometries and boundary conditions, it is possible to find analytical solutions of (1). For example, in a concentric configuration having isothermal surfaces with internal and external radii r_i and r_o, respectively (see Figure 1), the conduction heat transfer is given by:

$$q_{cond} = 2\pi k_{air} \frac{T_i - T_o}{ln\frac{r_o}{r_i}} = h_c(T_i - T_o) \tag{2}$$

where h_c is the corresponding heat transfer coefficient.

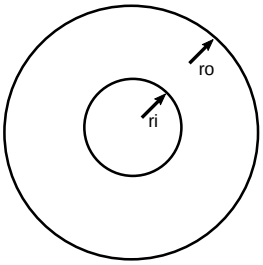

Figure 1. Cable inside a pipe/tube.

Heat transport by natural or forced convection is caused by heating of a fluid which flows over a surface, and the flow then carries the heat away. In the annulus formed by cable and J-tube, natural convection occurs as at the cable surface air is heated and flows upwards and at the J-tube inner surface air is cooled and flows downwards. This effect can be included in an overall effective heat transfer coefficient *h*. The radiation in the annulus is also in the same overall heat transfer coefficient. On the outside surface of a circular cylinder with a cross flow wind the heat transfer coefficient h_c is then a function of the pipe dimensions and the wind speed (through the Reynolds number Re_D)

$$q = h_c\left(T_{surface} - T_{air}\right) \tag{3}$$

From the outside of the J-tube there is also radiation of heat to the surroundings at ambient conditions. In addition to the heat generated by the load current in the cable there is an external heat source due the solar radiation that hits the external surface of the J-tube (and cable if the cable is exposed), as shown in Figure 2. The magnitude of the solar radiation is primarily given by the maximum solar radiosity but is reduced by clouds and particles that absorbs and scatters radiation. The effective solar radiation magnitude is determined by the exposed area normal to the radiation direction.

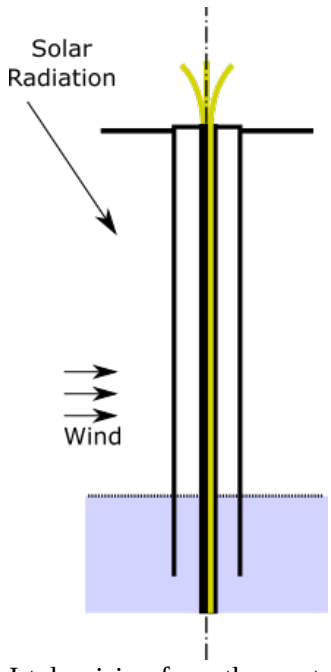

Figure 2. Cable in J-tube rising from the sea to the deck hang-off.

3. Ampacity calculation methods

The party performing the ampacity calculations vary on a project basis, depending on sales contract structure. It can be conducted by the installation contractor, the power cable or core vendor, or a subcontractor of any of these. Also, a 3rd party verification is often conducted initiated by the operator of the cable. Calculations are either performed by IEC standards, or by FEM. Their function, advantages and disadvantages are outlined in the next sub-sections.

3.1 IEC

The main standard for ampacity calculations is IEC 60287 [2]. Ampacity calculations applying IEC 60287 are based on a combination of analytical formulas and simplified empirical expressions describing heat generation and dissipation for most cable types and relevant laying geometries. Performing such calculations by hand, in spreadsheets or scripts is time-consuming and complicated, especially for cable circuits involving many cables. As IEC 60287 does not cover all thermal bottlenecks, supplements such as [8] are needed for correct calculations of the entire routing. The cable and power core vendors have often developed software based on the IEC formulas for their cable design, and therefore often prefer this option.

3.2 FEM

Computations of ampacity with FEM are becoming more commonly used for ampacity calculations, due to increased availability of computational power and user friendliness of software solutions. The major advantage of using FEM is that constraints on cable trench geometries in IEC 60287 does not apply. Comparison of published FEM solutions to IEC 60287 calculations for buried cables show generally good agreement [9], [10]. For cable laying geometries including convection as heat transport mechanism, good agreement to real cases, and in line with analytical solutions, is found using FEM [11]. For larger and more complex structures, such as duct banks, increasing discrepancy is found with increasing number of cables, due to the simplifications of electromagnetic couplings in the IEC standard.

4. Setup of FEM procedure

The finite element model is built assuming a generic 72.5 kV 800 mm^2 armoured triad cable. Each cable has a 20 mm^2 screen. The cross-section is shown in Figure 3, and geometric dimensions of cable and J-tube and material properties are summarized in Table A.1 while cable system electrical properties are given in Table A.2. A balanced 3-phase current equal to 1130 A (rms) at 50Hz is applied to the conductors. The current in each armour wire is set to zero since the armour wires normally are twisted with a pitch different from the triad giving net zero induction.

The cable is placed in the centre of an air-filled J-tube, as shown in Figure 2. The air domain is for the purposes of this study assigned a thermal conductivity of 2 W/m·K. On the outer surface of the J-tube heat dissipates by radiation and convection to the surroundings. The convective heat transfer is applied by use of a heat transfer coefficient equal to 5 $W/m^2 \cdot K$ (no wind) or 60 $W/m^2 \cdot K$ (windy).

The time variation in incident solar heat flux as shown in Figure 4 is used in this study. This represents the incident radiation on a vertical cylindrical surface on Midsummer day at latitude 61N. The maximum value is 900 W/m^2 and occurs at 9 a.m. The 24-hour rms value is 576 W/m^2, and the 24-hour average value is 457 W/m^2.

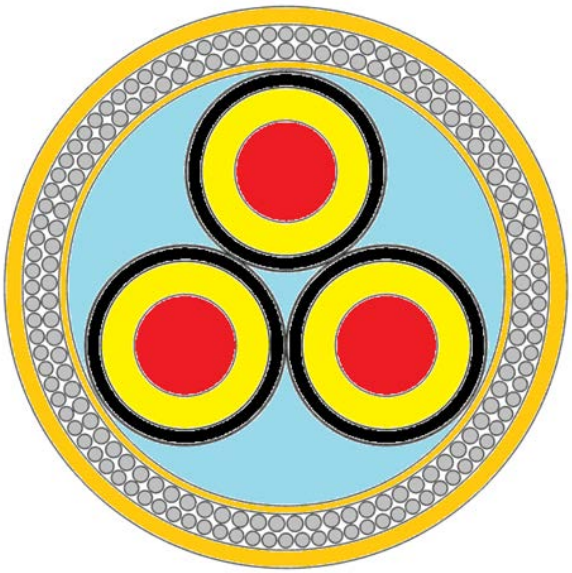

Figure 3. Model cable cross-section.

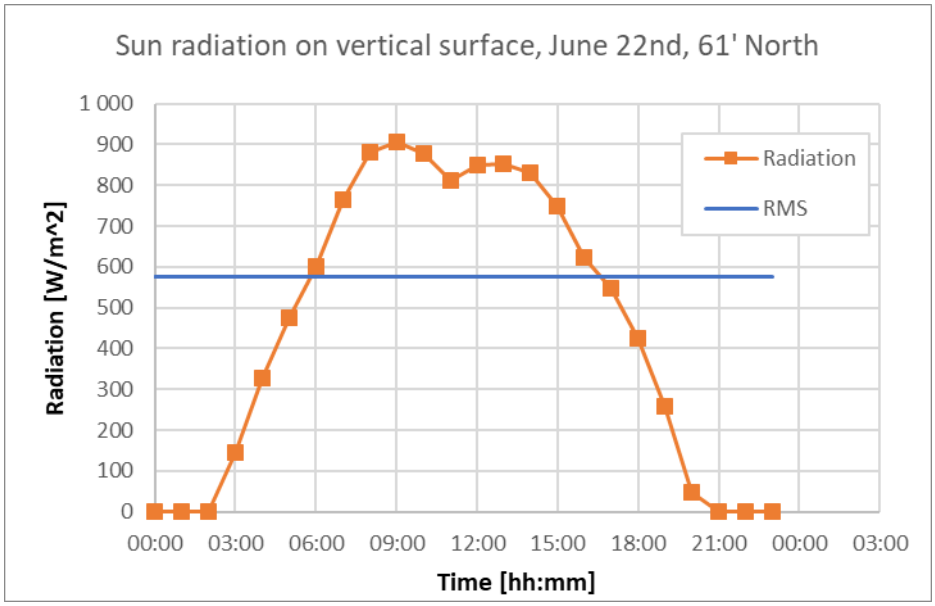

Figure 4. Incident solar flux on vertical pipe.

In the FEM model, the incident solar heat flux is applied as a heat source on the outer surface of the J-tube with three different approaches:

i) **RMS value** equal to 576 W/m^2. This value is homogeneously distributed over the entire circumference of the J-tube, i.e., at a value 576*D/πD=183 W/m^2 (D is J-tube diameter). From this, the steady-state temperature distribution is found.

ii) **Time-dependent** solar flux. In this approach, the incident solar flux is varied according to the orange line in Figure 4, homogeneously distributed on the J-tube circumference.

iii) **Time-dependent and directional** solar influx. In this case the solar flux is applied to the J-tube surface with an incident orientation that follows the sun during a 24-hour period, i.e. north (up) at midnight, South (down) at noon.

5. Results and discussion

The computed cable temperature field for the steady-state conditions using the RMS value of the solar influx is shown in Figure 5. The conductor temperature is 90 ºC, which is typically considered the threshold level for XLPE cables. This approach suggests that 1130 A is the ampacity of the system, or alternatively, that a larger conductor cross-section should be selected if the production is expected to be higher.

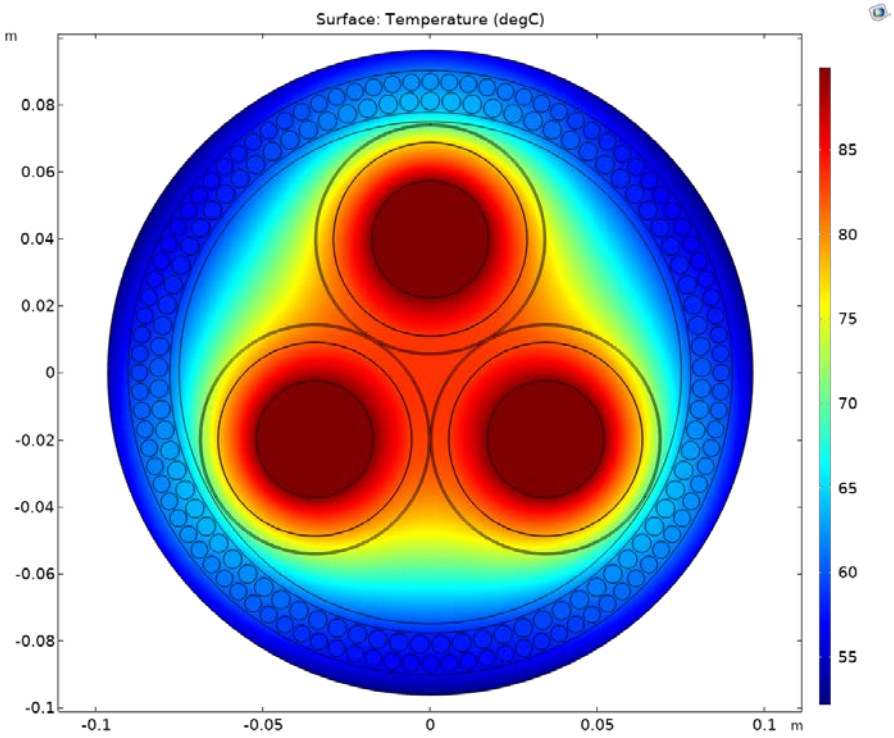

Figure 5. Temperature distribution in cable.

When time-varying solar influx is considered, the conductor temperature rises and decreases with the sun, thus oscillating between 78 ºC and 94 ºC. The hourly variation in conductor temperature for this approach is shown in Figure 6 with a grey line, while the conductor temperature for constant solar flux is shown as straight blue line as reference. Due to the large thermal mass of the system, there is a lag between the magnitude of the incident flux and the conductor temperature. The solar influx is maximum between 8 a.m. and 2 p.m., whereas the maximum conductor temperature occurs about 5 p.m. Since the maximum temperature now exceeds 90 ºC, the model suggests that the current rating must be reduced to avoid overheating the insulation material.

For the third approach, where the direction of the incident solar radiation is included, the conductor temperature increases further to a maximum value of 95 ºC, as shown by the orange line in Figure 6. At approximately 2 p.m. there is a break in the temperature curve; this is due to the maximum temperature shifting from the lower right cable to the lower left cable as the sun moves west.

In wind farms, periods of high load will always coincide with wind. This wind will have a cooling effect on the J-tube surface. To account for this, the heat transfer coefficient is increased from 5 to 60 W/m^2 K on the J-tube surface, which are reference values for windless and winds at 20 m/s, respectively [12]. The increased cooling effect gives a significant decrease in temperature, reducing the maximum value from 95 ºC to 72 ºC, as shown by the yellow line in Figure 6. Hence, the model now shows that the cable

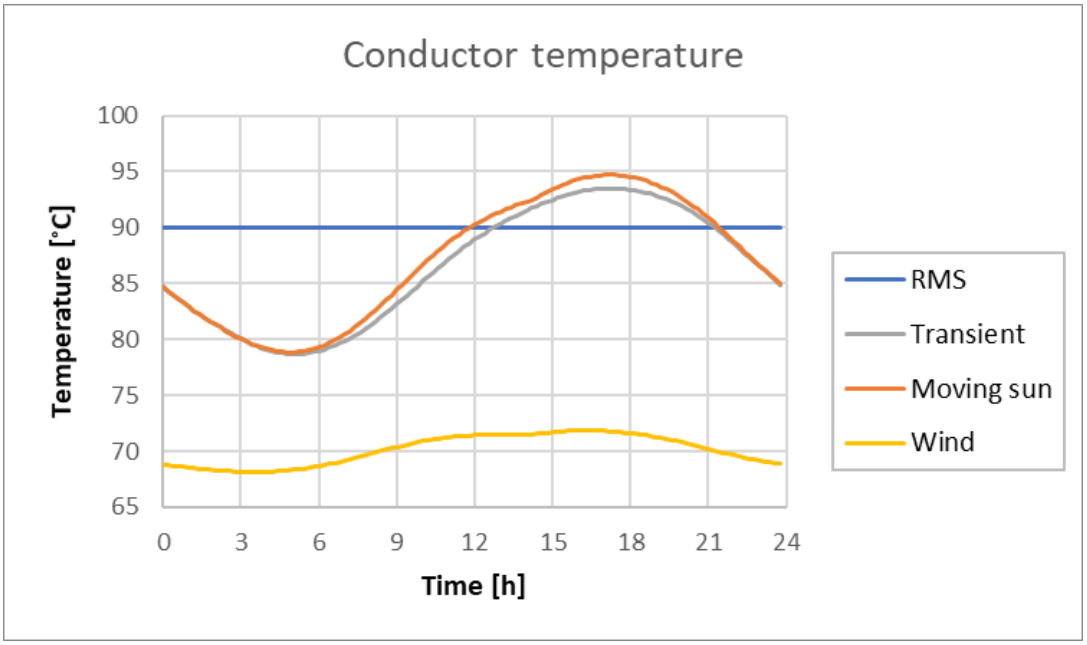

Figure 6. Conductor temperature for the different modelling cases.

is in no danger of being overheated. By redoing the calculations, it can now be found that the 800 mm^2 cable can carry 1330 A, an increase of 17%, when both moving solar influx and wind is taken into account – thus demonstrating the benefit of including more advanced description of environmental parameters.

If the ampacity limit for the cable is met by the calculations with a large margin, a smaller conductor size can be considered. To illustrate this case, a scaled down cable with cross-section of 630 mm^2 have been modelled, taking into account moving solar influx and wind. In Figure 7 the conductor temperature is shown as an orange line for the 630 mm^2 cable and the 800 mm^2 as a yellow line. The maximum conductor temperature is now 84 ºC, well below the limit of 90 ºC.

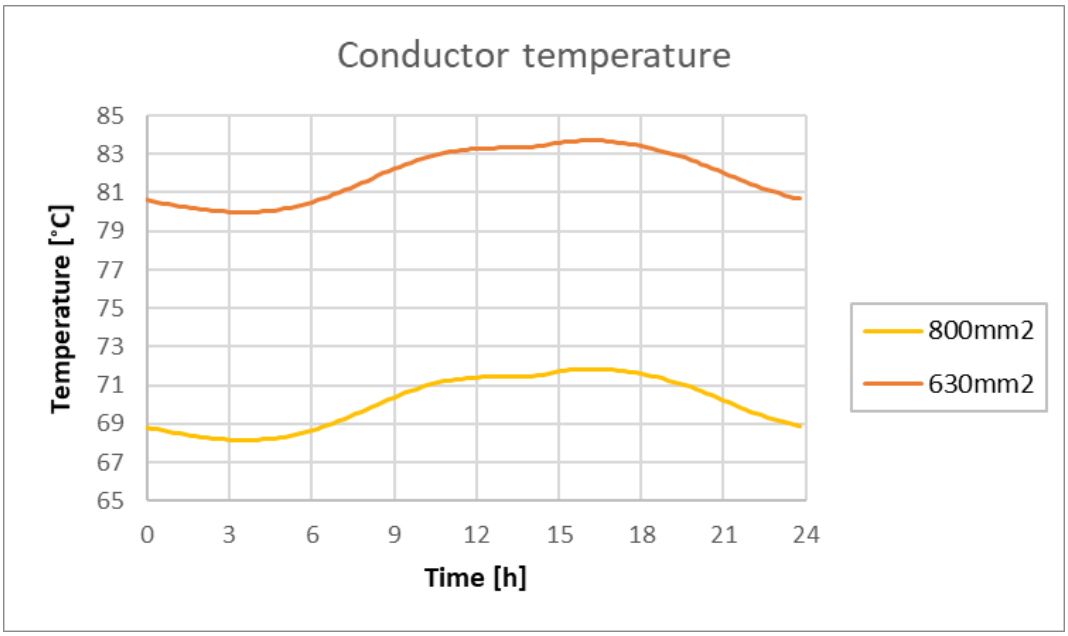

Figure 7. Conductor temperature for cross-section areas 630 and 800 mm^2 with wind cooling.

6. Summary

In this work FEM have been applied to calculate the ampacity of a three-core HV cable situated in a J-tube – a normal laying geometry in offshore wind turbines where the cable goes from tower to sea. It was found that taking into account the trajectory of solar influx, the maximum temperature increased above the admittable cable core temperature. In this calculation wind-still was assumed giving too low heat dissipation from J-tube surface to surrounding, as there high cable loads always will coincide with wind and thus increased heat transfer coefficient. By taking this into account it was found the highest core cable temperature decreased by 18 ^{o}C compared to the steady-state case. These more accurate ampacity calculations can be exploited by either increasing the admissible current in the cable by 17% or decreasing the cable cross section thus reducing CAPEX significantly.

Future work should focus on verification with temperature, load and weather data from real installations.

Acknowledgements

This publication has been prepared as part of NorthWind (Norwegian Research Centre on Wind Energy) co-financed by the Research Council of Norway, industry, and research partners. Read more at www.northwindresearch.no.

Appendix

Construction and material parameters used in this study is given in Tables A1 and electrical properties are given in Table A2.

Table A.1. Properties of 72.5 kV 800 mm^2 and 630 mm^2 type cables and J-tube used in calculations.

Geometry	Material	Thermal conductivity (W/m.K)	Heat capacity (MJ/m^3.K)	Diameter 800 mm^2 (mm)	Diameter 630 mm^2 (mm)
Conductor	Copper	385	3.45	35	31
Insulation	XLPE	0.286	2.5	57.8	53.8
Screen	Copper	385	3.45	58	54
Inner sheath	S.C PE	0.286	2.5	68	64
Armour	Steel	20	3.8	179	175
Serving	PE	0.286	2.5	193	189
Interstices	-	0.286	2.5	-	-
J-tube inner radius	Steel	100	3.3	514	514
J-tube outer radius				559	559
	Air	2	0.001		

Table A.2. Cable system electrical properties.

Parameter	Value
Fill factor	0.8
Conductor conductivity	58e6 S/m
Screen conductivity	58e6 S/m
Armour conductivity	1.4e6 S/m
Armour relative magnetic permeability	100
J-tube conductivity	1.3e6 S/m
Frequency	50 Hz

References

[1] IEA 2019 Offshore Wind Outlook 2019 (https://www.iea.org/reports/offshore-wind-outlook-2019)

[2] International Electrotechnical Commission 2006 IEC 60287 - Electric Cables - Calculation of the Current Rating

[3] International Electrotechnical Commission 1989 IEC 60853-2: Calculation of the cyclic and emergency current rating of cables. Part 2: Cyclic rating of cables greater than 18/30 (36) kV and emergency ratings for cables of all voltages

[4] Kvarts T, Arana I, Olsen R and Mortensen P 2016 *CIGRE Session (Paris)* Systematic Description of Dynamic Load for Cables Offshore Wind Fars, Method and Experience **B1-303**

[5] Catmull S, Chippendale R D, Pilgrim J A, Hutton G and Cangy P 2016 *IEEE Transactions on Power Delivery* Cyclic Load Profiles for Offshore Wind Farm Cable Rating **31** p 1242

[6] National Center for Atmospheric Research 2022 *WEATHER RESEARCH AND FORECASTING MODEL* (https://www.mmm.ucar.edu/weather-research-and-forecasting-model)

[7] Chippendale R D, Pilgrim J A, Goddard K F and Cangy P 2017 *IEEE Transactions on Power Delivery* Analytical Thermal Rating Method for Cables Installed in J-Tubes **32** p 1721

[8] Anders G 2005 *Rating of Electric Power Cables in Unfavorable Thermal Environment* (New York: John Wiley & Sons Inc)

[9] Dubitsky S, Greshnyakov G and Korovkin N 2016 *IEEE International Energy Conference (Leuven)* Comparison of Finite Element Analysis to IEC-60287 for Predicting Underground Cable Ampacity

[10] Swaffield D, Lewin P and Sutton S 2008 *IET Generation, Transmission and Distribution* Methods for rating directly buried high voltage cable circuits **2** p 393

[11] Hellesø S M and Eberg E 2021 *IEEE Transactions on Power Delivery* Simplified model for heat transport for cables in pipes *preprint* 10.1109/TPWRD.2021.3137876

[12] Shitzer A 2006 *International journal of biometeorology* Wind-chill-equivalent temperatures: Regarding the impact due to the variability of the environmental convective heat transfer coefficient **50** p 224